



Published in final edited form as:

Nature. ; 480(7375): 63–68. doi:10.1038/nature10658.

Mutations causing syndromic autism define an axis of synaptic pathophysiology

Benjamin D. Auerbach, Emily K. Osterweil, and Mark F. Bear

Howard Hughes Medical Institute, The Picower Institute for Learning and Memory, Department of Brain and Cognitive Sciences, Massachusetts Institute of Technology Cambridge MA, 02139, USA

Summary

Tuberous sclerosis complex and fragile X syndrome are genetic diseases characterized by intellectual disability and autism. Because both syndromes are caused by mutations in genes that regulate protein synthesis in neurons, it has been hypothesized that excessive protein synthesis is one core pathophysiological mechanism of intellectual disability and autism. Using electrophysiological and biochemical assays of neuronal protein synthesis in the hippocampus of *Tsc2*^{+/-} and *Fmr1*^{-/-} mice, we show that synaptic dysfunction caused by these mutations actually falls at opposite ends of a physiological spectrum. Synaptic, biochemical and cognitive defects in these mutants are corrected by treatments that modulate metabotropic glutamate receptor 5 in opposite directions, and deficits in the mutants disappear when the mice are bred to carry both mutations. Thus, normal synaptic plasticity and cognition occur within an optimal range of metabotropic glutamate receptor-mediated protein synthesis, and deviations in either direction can lead to shared behavioral impairments.

Introduction

Greater than 1% of the human population has an autism spectrum disorder (ASD), and it has been estimated that over 50% of those with autism also have intellectual disability (ID)¹. In the large majority of cases, the cause is unknown. However, genetically defined syndromes with increased prevalence of autism and ID offer an opportunity to understand the brain pathophysiology that manifests as ASD and ID, and this knowledge can suggest potential therapies. A case in point is fragile X syndrome (FXS), caused by silencing of the *FMR1* gene and loss of the protein product, FMRP. Studies of the *Fmr1* knockout (-/-) mouse revealed that in the absence of FMRP, protein synthesis is increased downstream of metabotropic glutamate receptor 5 (mGluR5). Diverse mutant phenotypes in fragile X animal models have been corrected by genetic or pharmacological inhibition of mGluR5, and preliminary human clinical trials using drugs that inhibit mGluR5 have shown promise². Because several other syndromic forms of ASD and ID are associated with mutations of genes that regulate mRNA translation at synapses, it has been hypothesized that altered synaptic protein synthesis might contribute generally to the autistic phenotype including ID³. The aim of the current study was to test the hypothesis that a mutation responsible for

Correspondence and requests for materials should be addressed to mbear@mit.edu.

Supplementary Information is linked to the online version of the paper at www.nature.com/nature

Authors Contributions M.F.B designed, directed and coordinated the project. B.D.A designed and performed electrophysiological recordings and behavior tests. E.O designed and performed biochemistry experiments.

Author Information Reprints and permissions information is available at www.nature.com/reprints. Mark Bear has a financial interest in Seaside Therapeutics, Inc.

another genetic syndrome associated with ASD and ID—tuberous sclerosis complex (TSC)—produces abnormalities in synaptic protein synthesis and plasticity similar to fragile X. If this were the case, treatments developed for one disorder might be beneficial for the other, and possibly for autism and ID more broadly.

The choice of TSC was guided by several considerations. Like FXS, (1) TSC is a single-gene disorder with core symptoms of ASD and ID, (2) the affected gene(s) lie in a signaling pathway that couples cell surface receptors to mRNA translation, (3) there are well validated mouse models of the disease, and (4) some mutant phenotypes in these mouse models have responded to pharmacological treatments that affect protein synthesis^{4–6}. The disease is caused by heterozygous mutations in the genes encoding TSC1 or TSC2 proteins that together form the TSC1/2 complex. TSC1/2 acts to inhibit Rheb, a Ras family GTPase with high specificity for mTOR within a protein complex called mTORC1. Rheb activation of mTORC1 can stimulate mRNA translation and cell growth, and excessive mTORC1 activation is believed to be pathogenic in TSC⁷. TSC is characterized by the growth of hamartomas that are believed to result from inactivation of the functional allele within the tumor cells^{8,9}. Although some neurological manifestations of TSC are thought to be related to tumor growth in the cerebral cortex, others including cognitive impairment and autism have been proposed to result from abnormal signaling at synapses¹⁰. Consistent with this idea, mice engineered to carry heterozygous loss-of-function mutations in *Tsc1* or *Tsc2* have been shown to have hippocampus-dependent learning and memory deficits without having tumors in the brain or seizures^{4,11}. Here we chose the *Tsc2*^{+/-} mouse model because *TSC2* mutations are more common and produce a more severe phenotype in humans¹², and this animal model is in widespread use^{4,13–15}. Of particular significance, postnatal treatment of *Tsc2*^{+/-} mice with the mTORC1 inhibitor rapamycin was previously shown to ameliorate hippocampal memory impairments suggesting the exciting possibility that some aspects of TSC, like FXS, might be amenable to drug therapy⁴.

A prominent hypothesis is that synaptic dysfunction in TSC relates to increased protein synthesis in response to elevated mTORC1 activity¹⁶. Signaling via mTORC1 has been suggested to contribute to the coupling of mGluR5 to protein synthesis and, although still controversial, it has been proposed that elevated mTOR activity might also be a cause of elevated protein synthesis in the *Fmr1*^{-y} mouse¹⁷. A sensitive electrophysiological read-out of local mRNA translation in response to mGluR5 activation is long-term synaptic depression (LTD) in area CA1 of the hippocampus^{18,19}. Indeed, it was exaggerated LTD in the *Fmr1*^{-y} mouse that led to the mGluR theory of FXS^{20,21}. Therefore, to test the hypothesis of a shared pathophysiology between TSC and FXS, we first examined mGluR-LTD in the hippocampus of male *Tsc2*^{+/-} mice.

Results

LTD was induced by activation of group 1 (Gp1) mGluRs (mGluR 1 and 5) with the selective agonist DHPG ((R,S)-3,5-dihydroxyphenylglycine) in hippocampal slices¹⁹. Unexpectedly, we discovered that DHPG-induced LTD was deficient rather than enhanced in the hippocampus of *Tsc2*^{+/-} mice, as compared to WT controls (Fig 1A). A similar deficit was observed when mGluR-LTD was induced by patterned electrical stimulation of Schaffer collateral synapses (Fig 1B). In agreement with a previous report⁴, basal synaptic transmission in CA1 appeared normal in the *Tsc2*^{+/-} mice, indicating that the impairment in mGluR-LTD is not due to general disruption of synaptic function (supplementary figure S1). Moreover, there was no difference in the magnitude of the NMDA receptor dependent form of LTD between WT and *Tsc2*^{+/-} mice (Fig 1C) demonstrating that the deficit is specific to mGluR-LTD, as these same synapses are able to undergo activity-induced depression via a different mechanism. To test the possibility of a general disruption in Gp 1 mGluR function,

we examined DHPG induced phosphorylation of extracellular signal-regulated kinase 1/2 (ERK1/2), a common measure of Gp1 mGluR signaling and a critical step for mGluR-mediated protein synthesis and LTD^{22,23}. Basal ERK1/2 phosphorylation and DHPG-induced increases in ERK1/2 phosphorylation are unaltered in *Tsc2*^{+/-} mice (Fig 1D). These results suggest that the deficit in mGluR-LTD seen in the *Tsc2*^{+/-} hippocampus is not due to a global dysregulation of synaptic function or Gp 1 mGluR signaling.

mGluR-LTD in area CA1 of the hippocampus is expressed via two independent mechanisms: reduced probability of presynaptic glutamate release²⁴⁻²⁶ and reduced expression of postsynaptic AMPA receptors^{25,27}. In WT animals, the postsynaptic modification is known to require immediate translation of mRNAs available in the dendrites of hippocampal pyramidal neurons^{18,28}. Accordingly, we found that LTD in WT mice at the age range examined (postnatal day (P) 25-30) is reliably reduced by the protein synthesis inhibitor cycloheximide (60 μ M; Fig 2A). The presynaptic component of LTD was monitored by measuring paired-pulse facilitation (PPF), which showed a persistent increase following DHPG that reflects reduced probability of glutamate released at the presynaptic terminal²⁴⁻²⁶. Changes in PPF were not inhibited by cycloheximide (supplementary figure S2; Fig 2C), suggesting that residual LTD in the presence of the drug is expressed presynaptically. While LTD was reduced in *Tsc2*^{+/-} mice, the persistent PPF change after DHPG was no different than in WT, suggesting a deficient postsynaptic modification (supplementary figure S2; Fig. 2C). Indeed, unlike WT, cycloheximide treatment had no effect on LTD in the *Tsc2*^{+/-} animals (Fig 2B). These data suggest a selective loss of the protein synthesis-dependent component of LTD in the mutant mice.

These electrophysiological results in the *Tsc2*^{+/-} hippocampus stand in stark contrast to the *Fmr1*^{-y} mouse in which mGluR-LTD is exaggerated²⁰. In the fragile X mouse model, increased LTD correlates with an increased rate of basal mRNA translation downstream of mGluR5. Therefore we were compelled to examine protein synthesis in hippocampal slices from the *Tsc2*^{+/-} mouse as previously described for the *Fmr1*^{-y} mouse²³. Consistent with the mGluR-LTD findings, we found a small but significant decrease in ³⁵S-methionine/cysteine incorporation into protein under basal conditions in the hippocampus of *Tsc2*^{+/-} mice (Fig 2D). This finding suggested the possibility that protein(s) required for mGluR-LTD are deficiently translated in the hippocampus of *Tsc2*^{+/-} mice. To test this idea we examined levels of Arc, a plasticity related protein that is rapidly synthesized in response to Gp 1 mGluR activation and is required for mGluR-LTD^{29,30}. Interestingly, we found that Arc expression is decreased in *Tsc2*^{+/-} hippocampal slices (Fig 2E). To determine whether this decrease was due to diminished translation, we measured the amount of newly-synthesized Arc in *Tsc2*^{+/-} slices by performing immunoprecipitation experiments on metabolically-labeled slices (see Methods)²³. Examination of the ³⁵S-incorporated fraction revealed a significant reduction in Arc translation in the hippocampus of *Tsc2*^{+/-} mice (Fig 2F). Control immunoprecipitations using non-immune IgG confirmed that our measurements were specific for Arc (supplementary figure S4). These results suggest that mGluR-LTD is deficient in the *Tsc2*^{+/-} hippocampus due to a decrease in the translation of the proteins required to stabilize LTD, including Arc.

As in the human disease, the germ line mutation in *Tsc2* can have myriad secondary consequences on neural development that could contribute to the observed LTD and protein synthesis phenotypes. To test the hypothesis that the deficient mGluR-LTD seen in *Tsc2*^{+/-} mice is a specific consequence of unregulated mTOR activity, we examined the effects of the mTORC1 inhibitor rapamycin. We found that acute rapamycin treatment (20 nM) restored mGluR-LTD in the *Tsc2*^{+/-} mice to WT levels (Fig 2G), while this same treatment had no effect on mGluR-LTD in slices from WT mice (supplementary figure S3). This rescue is due specifically to the recovery of the protein synthesis-dependent component of

LTD, as the effect of rapamycin in *Tsc2*^{+/-} mice was eliminated in the presence of cycloheximide (Fig. 2H). The same rapamycin treatment also restored basal protein synthesis rates in *Tsc2*^{+/-} hippocampal slices back to WT levels (Fig. 2I). The simple model that best fits the data is that unregulated mTOR activity caused by the *Tsc2*^{+/-} mutation suppresses the protein synthesis that is required for mGluR-LTD (Fig 3A).

In the *Fmr1*^{-/-} model of FXS, excessive mGluR-LTD and hippocampal protein synthesis can be corrected by reducing signaling via mGluR5^{23,31}. We therefore wondered if the opposite approach of potentiating mGluR5 signaling with a positive allosteric modulator (PAM) could be beneficial in this model of TSC (Fig 3A). PAMs are compounds that do not activate mGluR5 directly but act on an allosteric site to potentiate physiological activation of the receptor³². Indeed, we found that pretreatment of hippocampal slices with the mGluR5 PAM 3-Cyano-N-(1,3-diphenyl-1H-pyrazol-5-yl)benzamide (CDPPB³³) restored the magnitude of mGluR-LTD in *Tsc2*^{+/-} mice to WT levels (Fig 3B). The rescue of LTD appears to be due specifically to recovery of the protein synthesis-dependent component because the effect of CDPPB was completely eliminated by cycloheximide (Fig 3C). Consistent with this conclusion, CDPPB treatment also restored basal protein synthesis levels (Fig 3D) and rescued the deficit in Arc synthesis in the *Tsc2*^{+/-} mice (Fig 3E). Thus, allosteric augmentation of mGluR5 signaling can overcome the inhibitory effect of unregulated mTOR activity on the synaptic protein synthesis that supports LTD.

In an important recent study, cognitive impairments in the *Tsc2*^{+/-} mice were shown to be significantly improved by treating the animals with the mTORC1 inhibitor rapamycin⁴. In light of our electrophysiological and biochemical findings, we wondered if a similar amelioration would be observed with the mGluR5 PAM. A robust phenotype was reported to be an impairment in the ability of the *Tsc2*^{+/-} mice to distinguish between familiar and novel contexts in a fear conditioning paradigm. Advantages of this paradigm are that the learning occurs in one trial making it amenable to acute drug treatment, and the memory is hippocampus-dependent³⁴. Although a requirement for CA1 LTD *per se* has not been established, contextual fear discrimination does depend on both mGluR5³⁵ and new protein synthesis at the time of training³⁶. In this assay, mice are first exposed to a distinctive context in which they receive an aversive foot shock. The next day, context discrimination is tested by dividing the animals into two groups; one is placed in the familiar context associated with the shock, and the other is placed in a novel context (Fig 3F). Context discrimination is assessed by measuring the time the animals express fear by freezing in each context. Although the WT mice clearly discriminate between contexts, the *Tsc2*^{+/-} mice do not⁴ (Fig 3G). To test the effect of augmenting mGluR5 signaling, mice from both genotypes were injected i.p. with CDPPB (10 mg/kg) 30 minutes prior to training. Although this treatment had no effect in the WT mice, it was sufficient to correct the deficit in context discrimination observed in the *Tsc2*^{+/-} mice. These results show that augmentation of mGluR5 signaling is beneficial at the behavioral level in *Tsc2*^{+/-} mice and that disrupted mGluR5 function may be relevant to cognitive impairments associated with TSC.

Contrary to our initial hypothesis we found that mutations causing FXS and TSC, two disorders associated with autism and ID, show mirror symmetrical alterations in protein synthesis-dependent LTD and have beneficial responses to treatments that modulate mGluR5 in opposite directions (Fig 4A). These findings raised the intriguing possibility that these two mutations could cancel one another on this functional axis. To test this hypothesis, we introduced an *Fmr1* deletion into the *Tsc2*^{+/-} background by crossing *Tsc2*^{+/-} males with *Fmr1*^{+/-} females (Fig 4B). This approach also enabled us to directly compare with WT the effects of the *Tsc2*^{+/-} and *Fmr1*^{+/-} mutations in littermates reared under identical conditions. As expected, mGluR-LTD was diminished in *Tsc2*^{+/-} mice and excessive in the

Fmr1^{-/-} mice, as compared to WT (Fig 4C,D). However, mice harboring both mutations showed mGluR-LTD that was indistinguishable from WT (Fig 4C,D).

While *Tsc2*^{+/-} and *Fmr1*^{-/-} mutations cause opposite alterations in mGluR-LTD and protein synthesis, the human disorders they are associated with have similar neurological and cognitive phenotypes. Might opposite deviations in synaptic function lead to shared cognitive impairments? To examine this question, we compared context discrimination in the *Tsc2*^{+/-} and *Fmr1*^{-/-} mice and discovered that indeed they do share a deficit in this measure of memory (Fig 4E). Remarkably, instead of being exacerbated, this memory deficit was erased in the double mutants (Fig 4E). These results suggest that the opposing synaptic deviations seen in *Tsc2*^{+/-} and *Fmr1*^{-/-} mice may manifest similarly at the behavioral level, as introducing both mutations not only reverses the disruptions of synaptic plasticity but rescues this memory impairment as well.

Discussion

LTD and protein synthesis downstream of mGluR5 have attracted attention in the context of several diseases, most notably FXS²⁷. Fragile X is caused by the loss of FMRP, an mRNA binding protein that negatively regulates translation^{37,38}. In the *Fmr1*^{-/-} mouse model, basal protein synthesis is elevated and LTD is exaggerated downstream of an mGluR5 signaling pathway involving ERK1/2²³. Partial inhibition of mGluR5 corrects multiple aspects of fragile X in animal models^{2,39}. Recent data suggest that the mTOR signaling pathway is also constitutively overactive in the *Fmr1*^{-/-} mouse¹⁷, but the relevance to exaggerated protein synthesis and altered synaptic function has been controversial. The current findings show that increased synaptic mTOR activity actually suppresses the protein synthesis required for LTD in the *Tsc2*^{+/-} mice. The idea that reduced protein synthesis is a causative factor in the observed deficit in synaptic plasticity is supported by the finding that pharmacological rescue with both rapamycin and CDPPB is abolished by cycloheximide, and the observation that Arc is deficiently translated in the *Tsc2*^{+/-} mice. There is good evidence that Arc is one of the proteins that normally must be synthesized to support mGluR5-dependent forms of long-term plasticity^{29,30}. Precisely how excess mTOR activity suppresses synthesis of these plasticity proteins remains to be investigated, but possibilities include hyperphosphorylation of FMRP⁴⁰ or increased translation of a competing pool of less abundant mRNAs unrelated to LTD^{7,21,30}. The fact that mGluR-LTD is altered in opposite directions in *Tsc2*^{+/-} and *Fmr1*^{-/-} mice, and that both deviations are corrected in the double mutants, suggests that the pool comprising LTD proteins is differentially regulated by FMRP and TSC1/2 (Fig. 3A).

The current findings also suggest a new treatment for behavioral deficits associated with TSC. Previous studies in the *Tsc2*^{+/-} mouse raised the exciting possibility that cognitive aspects of the disorder might be ameliorated with rapamycin, even when treatment is begun in adulthood⁴. Our data show that an mGluR5 PAM may be similarly effective. While rapamycin has been used clinically, it is problematic for chronic treatment because of its strong immunosuppressive properties. The benefit of mGluR5 PAMs is that they target specifically the synaptic mechanisms that are likely responsible for the cognitive and behavioral impairments in TSC.

TSC and FXS represent two leading genetic risk factors for ASD and ID⁴¹. Although great strides have been made in identifying genetic variation that correlates with non-syndromic autism, there is little known about ASD pathophysiology—knowledge that is essential for developing effective therapies. Our test of the hypothesis that the *Fmr1*^{-/-} and *Tsc2*^{+/-} models of FXS and TSC have a shared synaptic pathophysiology revealed instead that they are at opposite ends of a spectrum: the *Fmr1* mutation causes exaggerated synaptic protein synthesis and LTD that are corrected by inhibition of mGluR5³¹, whereas the *Tsc2* mutation

causes diminished synaptic protein synthesis and LTD that are corrected by augmentation of mGluR5 (Fig. 4A). Moreover, the opposing effects of these mutations balance one another at synaptic and behavioral levels in the double mutant. This finding is interesting in light of recent discoveries that gain- and loss-of-function mutations in individual genes, such as *MECP2*, can often yield syndromes with overlapping features, such as epilepsy, cognitive impairment, and ASD⁴². Our findings reveal that even genetically heterogeneous causes of ASD and ID may produce similar deficits by bidirectional deviations from normal on a common functional axis. The important implication is that therapies designed to correct one cause of ASD are not likely to be effective for all other causes, and might well be deleterious. It will be critical to understand where a patient lies on the spectrum of synaptic function to choose an appropriate therapy for ASD and other psychiatric disorders.

Methods Summary

For detailed methods, please see the Supplementary Information. All experimental procedures were approved by the MIT Institutional Animal Care and Use Committee. Age-matched, male littermate mice bred on the C57Bl/6J clonal background were used in this study. Acute hippocampal slices were prepared from P25-35 mice as previously described³¹ and field EPSPs (fEPSPs) evoked by stimulation of the Schaffer collaterals were recorded in CA1 *stratum radiatum* with extracellular electrodes. LTD was induced by applying R,S-DHPG (50 μ M) or S-DHPG (25 μ M) for 5 minutes, or by paired-pulse low frequency synaptic stimulation (PP-LFS)^{18,19} for 20 minutes. Metabolic labeling, immunoblotting, and immunoprecipitation experiments were performed on yoked WT and *Tsc2*^{+/-} mice as described previously^{23,43}. Context discrimination fear conditioning was performed as described previously⁴. For *in vivo* mGluR5 PAM experiments, animals received a single injection of CDPPB (10 mg/kg, i.p.) 30 minutes prior to the training session. For all data sets, outliers > 2 standard deviations from the mean were removed, and significance between more than two groups was determined using two-way ANOVA and *post-hoc* Student's *t*-tests. Statistics were performed using each animal as an "n", with each animal represented by the mean of 1–4 slices for electrophysiology experiments, 1 slice per animal for biochemistry experiments, and 5–8 slices per animal for IP experiments. All experiments were performed blind to genotype and include interleaved controls for genotype and treatment.

Materials and Methods

Animals

Tsc2^{+/-} male and female mutant mice on the C57Bl/6J clonal background were bred with C57Bl/6J WT partners to produce the WT and *Tsc2*^{+/-} male offspring used in this study. For genetic rescue experiments, heterozygous *Tsc2* male mice (*Tsc2*^{+/-}) were bred with heterozygous *Fmr1* females (*Fmr1* x⁺/x⁻), both on the C57Bl/6J clonal background, to obtain F1 male offspring of four genotypes: wild type (*Tsc2*^{+/+}, *Fmr1*^{+/y}), *Fmr1* KO (*Tsc2*^{+/+}, *Fmr1*^{-/y}), *Tsc2* Het (*Tsc2*^{+/-}, *Fmr1*^{+/y}), and Cross (*Tsc2*^{+/-}, *Fmr1*^{-/y}) (Fig. 4B). All experimental animals were age-matched male littermates, and were studied with the experimenter blind to genotype and treatment condition. Animals were group housed and maintained on a 12:12 hr light:dark cycle. The Institutional Animal Care and Use Committee at MIT approved all experimental techniques.

Electrophysiology

Acute hippocampal slices were prepared from P25-35 animals in ice-cold dissection buffer containing (in mM): NaCl 87, Sucrose 75, KCl 2.5, NaH₂PO₄ 1.25, NaHCO₃ 25, CaCl₂ 0.5, MgSO₄ 7, Ascorbic acid 1.3, and D-glucose 10 (saturated with 95% O₂/5% CO₂).

Immediately following slicing the CA3 region was removed. Slices were recovered in artificial cerebrospinal fluid (ACSF) containing (in mM): NaCl 124, KCl 5, NaH₂PO₄ 1.23, NaHCO₃ 26, CaCl₂ 2, MgCl₂ 1 and D-glucose 10 (saturated with 95% O₂/5% CO₂) at 32.5°C for ≥ 3 hours prior to recording.

Field recordings were performed in a submersion chamber, perfused with ACSF (2–3 ml/min) at 30 °C. Field EPSPs (fEPSPs) were recorded in CA1 *stratum radiatum* with extracellular electrodes filled with ACSF. Baseline responses were evoked by stimulation of the Schaffer collaterals at 0.033 Hz with a 2-contact cluster electrode (FHC) using a 0.2 ms stimulus yielding 40–60% of the maximal response. Field potential recordings were filtered at 0.1 Hz – 1 kHz, digitized at 10 kHz, and analyzed using pClamp9 (Axon Instruments). The initial slope of the response was used to assess changes in synaptic strength. Data were normalized to the baseline response and are presented as group means ± SEM. LTD was measured by comparing the average response 55–60 minutes post DHPG application to the average of the last 5 minutes of baseline.

The input output function was examined by stimulating slices with incrementally increasing current and recording the fEPSP response. Paired pulse facilitation was induced by applying two pulses at different interstimulus intervals. Facilitation was measured by the ratio of the fEPSP slope of stimulus 2 to stimulus 1. NMDAR-dependent LTD was induced by delivering 900 test pulses at 1 Hz. mGluR-LTD was induced by applying R, S-Dihydroxyphenylglycine (R,S-DHPG, 50 μM) or S-Dihydroxyphenylglycine (S-DHPG, 25 μM) for 5 minutes, or by delivering 1200 pairs of pulses (with a 50 ms interstimulus interval) at 1 Hz. In some experiments slices were incubated with the protein synthesis inhibitor cycloheximide (60 μM) for 30 minutes as follows: 20 minutes during baseline recording, 5 minutes during DHPG application and 5 minutes post DHPG application. For mGluR5 PAM experiments, slices were pretreated with CDPPB (10 μM) or DMSO control for 30 minutes in same manner as above, either in the presence of cycloheximide or control ACSF. For rapamycin experiments, slices were pretreated with rapamycin (20 nM) or DMSO control, with or without cycloheximide, for at least 30 minutes prior to recording and throughout the entire experiment. Significance was determined by two-way ANOVA and *post-hoc* Student's t-tests. Statistics were performed using each animal as an “n”, with each animal represented by the mean of 1–4 slices. All experiments were performed blind to genotype and include interleaved controls for genotype and treatment.

Metabolic labeling of new protein synthesis

Performed as described by Osterweil *et al*²³. Briefly, 500 μm slices were recovered for 4 h in 32.5°C ACSF (in mM: 124 NaCl, 3 KCl, 1.25 NaH₂PO₄, 26 NaHCO₃, 10 dextrose, 1 MgCl₂, 2 CaCl₂, saturated with 95% O₂ and 5% CO₂), incubated for 30 min with 25 μM ActD ± rapamycin (20 nM) or CDPPB (10 μM), and transferred to fresh ACSF ± drug with 10 μCi/ml ³⁵S-Met/Cys (Perkin Elmer) for another 30 min. After labeling, slices were homogenized, and labeled proteins isolated by TCA precipitation. Samples were read with a scintillation counter and also subjected to a protein concentration assay (Bio-Rad). Final data were expressed as counts per minute (CPM) per μg protein, normalized to the ³⁵S-Met/Cys ACSF used for incubation, and the average incorporation of all samples analyzed in that experiment. For autoradiography, homogenized slices were processed for SDS PAGE, transferred to nitrocellulose, stained for total protein using the Memcode staining kit (Pierce), and ³⁵S-incorporated proteins visualized with the aid of a phosphorimager (Fujifilm).

Immunoblotting

Immunoblotting was performed according to established methods using primary antibodies to Arc (Synaptic Systems), p-ERK1/2 (Thr202/Tyr204) (Cell Signaling Technology) or ERK1/2 (Cell Signaling Technology). ERK1/2 phosphorylation was measured by densitometry (Quantity One), and quantified as the densitometric signal of p-ERK1/2 divided by the ERK1/2 signal in the same lane. To quantify Arc expression, the densitometric signal of Arc was divided by the total protein signal (determined by Memcode staining) in the same lane.

Immunoprecipitation

Hippocampal slices (5–8 per animal) were metabolically labeled with 50 $\mu\text{Ci/ml}$ ^{35}S -Met/Cys for 3 h, and immunoprecipitation (IP) performed on yoked WT and *Tsc2*^{+/-} slices essentially as described previously²³. Briefly, slices were homogenized in IP lysis buffer (Pierce) plus protease inhibitors (EMD Biosciences), spun at 16,000 \times g, and supernatants pre-cleared with protein A/G sepharose. To avoid contamination of the Arc signal with IgG heavy chain, immunoprecipitation was performed using columns of monoclonal Arc antibody (a generous gift from P. Worley) crosslinked to protein A/G sepharose (Pierce Crosslink IP Kit). Immunoprecipitated Arc was resolved on SDS PAGE gels, transferred to nitrocellulose, and exposed to a phosphorimager screen for 2–3 weeks. The same membranes were then immunoblotted for Arc. For each sample, the ratio of ^{35}S -incorporated: total was calculated by dividing the density of the band seen by autoradiography to the density of band seen by immunoblot (in the same lane).

Contextual Fear Conditioning

6–12 week old WT, *Tsc2*^{+/-}, *Fmr1*^{-y}, and Cross (*Tsc2*^{+/-} \times *Fmr1*^{-y}) mice were fear conditioned to the training context with one 0.8 mA shocks (2 sec) as described by Ehninger *et al*⁴. The mice were allowed 3 minutes to explore context before conditioning and were removed 15 sec after the shock was given and returned to home cage. Conditioned fear response was assessed 24 hours later by a trained observer blind to condition, measuring the percentage of time spent freezing during the test period (3 min session). To determine context specificity of the conditioned response, mice trained at the same time were separated into two groups: one group was tested in the same training context and the other tested in a novel context. This novel context was created by varying: distal cues, odor (2% acetic acid vs. 70% ethanol), floor material (plastic vs. metal bars), and lighting (red vs. white) of the testing apparatus. For rescue experiments, animals received a single injection of CDPPB (10 mg/kg, i.p.) 30 minutes prior to training session.

Reagents

(R,S)-3,5-dihydroxyphenylglycine (R,S-DHPG) was purchased from Tocris Biosciences (Ellisville, MO) and (S)-3,5-dihydroxyphenylglycine (S-DHPG) was purchased from Sigma (St. Louis, MO). Fresh bottles of DHPG were prepared as a 100x stock in H₂O, divided into aliquots, and stored at -80°C. Fresh stocks were made once a week. Rapamycin (EMD Biosciences, San Diego, CA) was prepared at 10 mM stock in DMSO and stored at -80°C. Final concentration of rapamycin was 20 nM in < 0.01% DMSO. Cycloheximide (Sigma) was prepared daily at 100x stock in H₂O. For slice experiments, 3-Cyano-N-(1,3-diphenyl-1H-pyrazol-5-yl)benzamide (CDPPB, EMD Biosciences) was prepared daily at 75 mM stock in DMSO with 0.5% bovine serum albumin (BSA) and diluted in ACSF to achieve final concentration of 10 μM in < 0.1% DMSO. For *in vivo* experiments, CDDPB was suspended in a vehicle consisting of 20% (2-Hydroxypropyl)-(R)-cyclodextrin in sterile saline. All other reagents were purchased from Sigma.

Supplementary Material

Refer to Web version on PubMed Central for supplementary material.

Acknowledgments

This work was partly supported by grants from the National Institute of Mental Health (T32 MH-082718 and T32-MH-074249), the National Institute of Child Health & Human Development (2R01HD046943), the Department of Defense (W81XWH-11-1-0252), and The Simons Foundation. We wish to acknowledge Dr. Arnold Heynen for advice and comments as well as Kathleen Oram, Erik Sklar, and Suzanne Meagher for technical and administrative assistance. Monoclonal Arc antibody was a generous gift from Paul Worley.

References

1. Newschaffer CJ, et al. The epidemiology of autism spectrum disorders. *Annu Rev Public Health*. 2007; 28:235–258. [PubMed: 17367287]
2. Krueger DD, Bear MF. Toward fulfilling the promise of molecular medicine in fragile X syndrome. *Annu Rev Med*. 2011; 62:411–429. [PubMed: 21090964]
3. Kelleher RJ 3rd, Bear MF. The autistic neuron: troubled translation? *Cell*. 2008; 135:401–406. [PubMed: 18984149]
4. Ehninger D, et al. Reversal of learning deficits in a *Tsc2*^{+/-} mouse model of tuberous sclerosis. *Nat Med*. 2008; 14:843–848. [PubMed: 18568033]
5. Meikle L, et al. Response of a neuronal model of tuberous sclerosis to mammalian target of rapamycin (mTOR) inhibitors: effects on mTORC1 and Akt signaling lead to improved survival and function. *J Neurosci*. 2008; 28:5422–5432. [PubMed: 18495876]
6. Onda H, et al. *Tsc2* null murine neuroepithelial cells are a model for human tuber giant cells, and show activation of an mTOR pathway. *Mol Cell Neurosci*. 2002; 21:561–574. [PubMed: 12504590]
7. Ehninger D, de Vries PJ, Silva AJ. From mTOR to cognition: molecular and cellular mechanisms of cognitive impairments in tuberous sclerosis. *J Intellect Disabil Res*. 2009; 53:838–851. [PubMed: 19694899]
8. Carbonara C, et al. 9q34 loss of heterozygosity in a tuberous sclerosis astrocytoma suggests a growth suppressor-like activity also for the *TSC1* gene. *Hum Mol Genet*. 1994; 3:1829–1832. [PubMed: 7849708]
9. Green AJ, Smith M, Yates JR. Loss of heterozygosity on chromosome 16p13.3 in hamartomas from tuberous sclerosis patients. *Nat Genet*. 1994; 6:193–196. [PubMed: 8162074]
10. de Vries PJ, Howe CJ. The tuberous sclerosis complex proteins—a GRIPP on cognition and neurodevelopment. *Trends Mol Med*. 2007; 13:319–326. [PubMed: 17632034]
11. Goorden SM, van Woerden GM, van der Weerd L, Cheadle JP, Elgersma Y. Cognitive deficits in *Tsc1*^{+/-} mice in the absence of cerebral lesions and seizures. *Ann Neurol*. 2007; 62:648–655. [PubMed: 18067135]
12. Cheadle JP, Reeve MP, Sampson JR, Kwiatkowski DJ. Molecular genetic advances in tuberous sclerosis. *Hum Genet*. 2000; 107:97–114. [PubMed: 11030407]
13. Onda H, Lueck A, Marks PW, Warren HB, Kwiatkowski DJ. *Tsc2*(^{+/-}) mice develop tumors in multiple sites that express gelsolin and are influenced by genetic background. *J Clin Invest*. 1999; 104:687–695. [PubMed: 10491404]
14. Nie D, et al. *Tsc2*-Rheb signaling regulates EphA-mediated axon guidance. *Nat Neurosci*. 2010; 13:163–172. [PubMed: 20062052]
15. Young DM, Schenk AK, Yang SB, Jan YN, Jan LY. Altered ultrasonic vocalizations in a tuberous sclerosis mouse model of autism. *Proc Natl Acad Sci U S A*. 2010; 107:11074–11079. [PubMed: 20534473]
16. Hoeffer CA, Klann E. mTOR signaling: at the crossroads of plasticity, memory and disease. *Trends Neurosci*. 2010; 33:67–75. [PubMed: 19963289]
17. Sharma A, et al. Dysregulation of mTOR signaling in fragile X syndrome. *J Neurosci*. 2010; 30:694–702. [PubMed: 20071534]

18. Huber KM, Kayser MS, Bear MF. Role for rapid dendritic protein synthesis in hippocampal mGluR-dependent long-term depression. *Science*. 2000; 288:1254–1257. [PubMed: 10818003]
19. Huber KM, Roder JC, Bear MF. Chemical induction of mGluR5- and protein synthesis--dependent long-term depression in hippocampal area CA1. *J Neurophysiol*. 2001; 86:321–325. [PubMed: 11431513]
20. Huber KM, Gallagher SM, Warren ST, Bear MF. Altered synaptic plasticity in a mouse model of fragile X mental retardation. *Proc Natl Acad Sci U S A*. 2002; 99:7746–7750. [PubMed: 12032354]
21. Bear MF, Huber KM, Warren ST. The mGluR theory of fragile X mental retardation. *Trends Neurosci*. 2004; 27:370–377. [PubMed: 15219735]
22. Gallagher SM, Daly CA, Bear MF, Huber KM. Extracellular signal-regulated protein kinase activation is required for metabotropic glutamate receptor-dependent long-term depression in hippocampal area CA1. *J Neurosci*. 2004; 24:4859–4864. [PubMed: 15152046]
23. Osterweil EK, Krueger DD, Reinhold K, Bear MF. Hypersensitivity to mGluR5 and ERK1/2 leads to excessive protein synthesis in the hippocampus of a mouse model of fragile X syndrome. *J Neurosci*. 2010; 30:15616–15627. [PubMed: 21084617]
24. Fitzjohn SM, et al. A characterisation of long-term depression induced by metabotropic glutamate receptor activation in the rat hippocampus in vitro. *J Physiol*. 2001; 537:421–430. [PubMed: 11731575]
25. Nosyreva ED, Huber KM. Developmental switch in synaptic mechanisms of hippocampal metabotropic glutamate receptor-dependent long-term depression. *J Neurosci*. 2005; 25:2992–3001. [PubMed: 15772359]
26. Mockett BG, et al. Calcium/calmodulin-dependent protein kinase II mediates group I metabotropic glutamate receptor-dependent protein synthesis and long-term depression in rat hippocampus. *J Neurosci*. 2011; 31:7380–7391. [PubMed: 21593322]
27. Luscher C, Huber KM. Group I mGluR-dependent synaptic long-term depression: mechanisms and implications for circuitry and disease. *Neuron*. 2010; 65:445–459. [PubMed: 20188650]
28. Snyder EM, et al. Internalization of ionotropic glutamate receptors in response to mGluR activation. *Nat Neurosci*. 2001; 4:1079–1085. [PubMed: 11687813]
29. Waung MW, Pfeiffer BE, Nosyreva ED, Ronesi JA, Huber KM. Rapid translation of Arc/Arg3.1 selectively mediates mGluR-dependent LTD through persistent increases in AMPAR endocytosis rate. *Neuron*. 2008; 59:84–97. [PubMed: 18614031]
30. Park S, et al. Elongation factor 2 and fragile X mental retardation protein control the dynamic translation of Arc/Arg3.1 essential for mGluR-LTD. *Neuron*. 2008; 59:70–83. [PubMed: 18614030]
31. Dolen G, et al. Correction of fragile X syndrome in mice. *Neuron*. 2007; 56:955–962. [PubMed: 18093519]
32. Conn PJ, Christopoulos A, Lindsley CW. Allosteric modulators of GPCRs: a novel approach for the treatment of CNS disorders. *Nat Rev Drug Discov*. 2009; 8:41–54. [PubMed: 19116626]
33. Kinney GG, et al. A novel selective positive allosteric modulator of metabotropic glutamate receptor subtype 5 has in vivo activity and antipsychotic-like effects in rat behavioral models. *J Pharmacol Exp Ther*. 2005; 313:199–206. [PubMed: 15608073]
34. Frankland PW, Cestari V, Filipkowski RK, McDonald RJ, Silva AJ. The dorsal hippocampus is essential for context discrimination but not for contextual conditioning. *Behav Neurosci*. 1998; 112:863–874. [PubMed: 9733192]
35. Lu YM, et al. Mice lacking metabotropic glutamate receptor 5 show impaired learning and reduced CA1 long-term potentiation (LTP) but normal CA3 LTP. *J Neurosci*. 1997; 17:5196–5205. [PubMed: 9185557]
36. Stiedl O, Palve M, Radulovic J, Birkenfeld K, Spiess J. Differential impairment of auditory and contextual fear conditioning by protein synthesis inhibition in C57BL/6N mice. *Behav Neurosci*. 1999; 113:496–506. [PubMed: 10443777]
37. Bassell GJ, Warren ST. Fragile X syndrome: loss of local mRNA regulation alters synaptic development and function. *Neuron*. 2008; 60:201–214. [PubMed: 18957214]

38. Darnell JC, et al. FMRP Stalls Ribosomal Translocation on mRNAs Linked to Synaptic Function and Autism. *Cell*. 2011; 146:247–261. [PubMed: 21784246]
39. Dolen G, Carpenter RL, Ocain TD, Bear MF. Mechanism-based approaches to treating fragile X. *Pharmacol Ther*. 2010; 127:78–93. [PubMed: 20303363]
40. Narayanan U, et al. S6K1 phosphorylates and regulates fragile X mental retardation protein (FMRP) with the neuronal protein synthesis-dependent mammalian target of rapamycin (mTOR) signaling cascade. *J Biol Chem*. 2008; 283:18478–18482. [PubMed: 18474609]
41. Fombonne E. Epidemiological surveys of autism and other pervasive developmental disorders: an update. *J Autism Dev Disord*. 2003; 33:365–382. [PubMed: 12959416]
42. Ramocki MB, Zoghbi HY. Failure of neuronal homeostasis results in common neuropsychiatric phenotypes. *Nature*. 2008; 455:912–918. [PubMed: 18923513]
43. Krueger DD, Osterweil EK, Bear MF. Activation of mGluR5 induces rapid and long-lasting protein kinase D phosphorylation in hippocampal neurons. *J Mol Neurosci*. 2010; 42:1–8. [PubMed: 20177824]

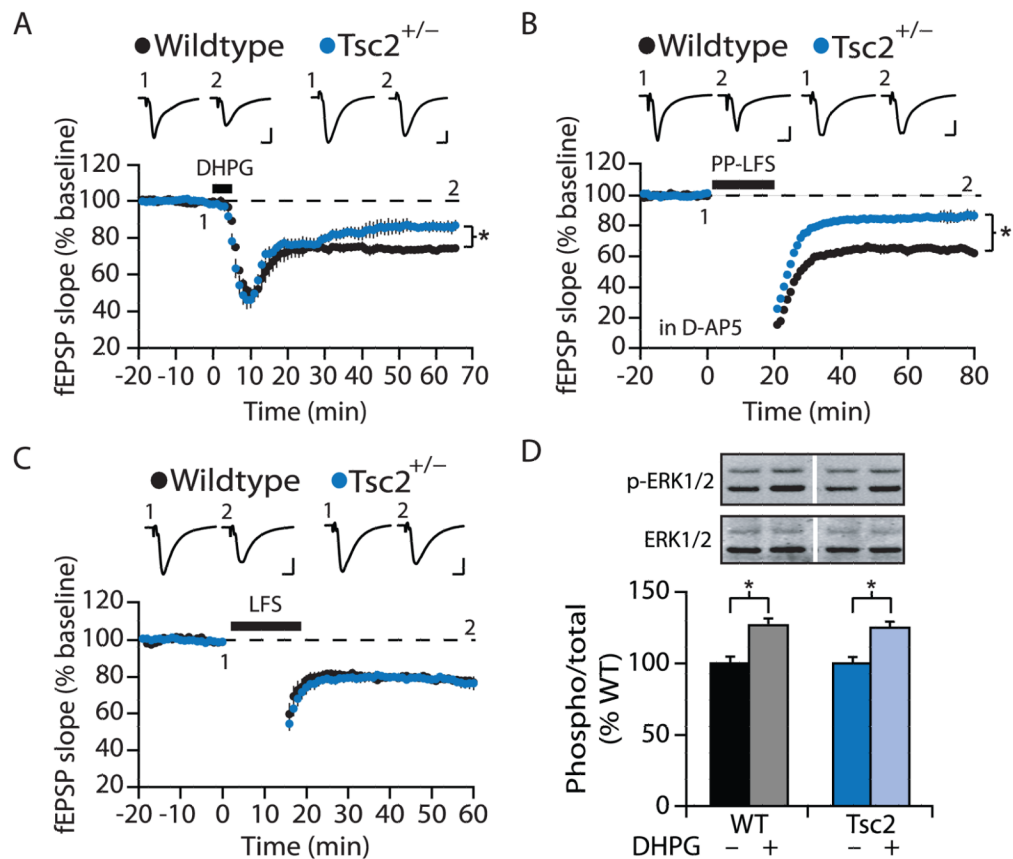


Figure 1. *Tsc2*^{+/-} mice have a specific deficit in mGluR-LTD

(A) DHPG induces significantly less LTD in slices from *Tsc2*^{+/-} mice vs. littermate WT mice (WT: $74.3 \pm 1.4\%$, $n = 5$ animals, 10 slices; *Tsc2*^{+/-}: $86.3 \pm 3.1\%$, $n = 6$ animals, 12 slices; * $p = 0.004$). In this and all subsequent electrophysiology figures, representative field potential traces (average of 10 sweeps) were taken at times indicated by numerals and scale bars equal 0.5 mV, 5 ms, unless stated otherwise. Error bars represent SEM. (B) Synaptically-induced mGluR-LTD, elicited by delivering pairs of pulses (50 ms interstimulus interval) at 1 Hz for 20 minutes (PP-LFS, 1200 pulses) in the presence of the NMDA receptor antagonist D-(–)-2-Amino-5-phosphonopentanoic acid (D-AP5, 50 μ M), is also deficient in slices from *Tsc2*^{+/-} mice (WT: $65.1 \pm 2.1\%$, $n = 3$ animals, 9 slices; *Tsc2*^{+/-}: $85.0 \pm 2.5\%$, $n = 4$ animals, 11 slices; * $p = 0.003$). (C) The magnitude of NMDA receptor-dependent LTD evoked by low frequency stimulation (LFS, 900 pulses at 1 Hz) does not differ between genotypes (WT: $79.8 \pm 1.6\%$, $n = 4$ animals, 6 slices; *Tsc2*^{+/-}: $79.4 \pm 1.9\%$, $n = 6$ animals, 6 slices; $p = 0.610$). (D) Hippocampal slices were stimulated with 50 μ M DHPG for 5 min, and ERK1/2 activation (phosphorylation) assessed via immunoblot (normalized WT: $100.0 \pm 6.1\%$, WT DHPG: $119.6 \pm 5.5\%$, *Tsc2*^{+/-}: $97.5 \pm 5.6\%$, *Tsc2*^{+/-} DHPG: $116.2 \pm 3.9\%$; ANOVA: genotype $p = 0.623$, treatment * $p = 0.0008$, genotype \times treatment $p = 0.923$; $n = 9$ animals). Results reveal that DHPG significantly increases ERK1/2 activation in both WT (* $p = 0.040$) and *Tsc2*^{+/-} (* $p = 0.003$). Error bars represent SEM.

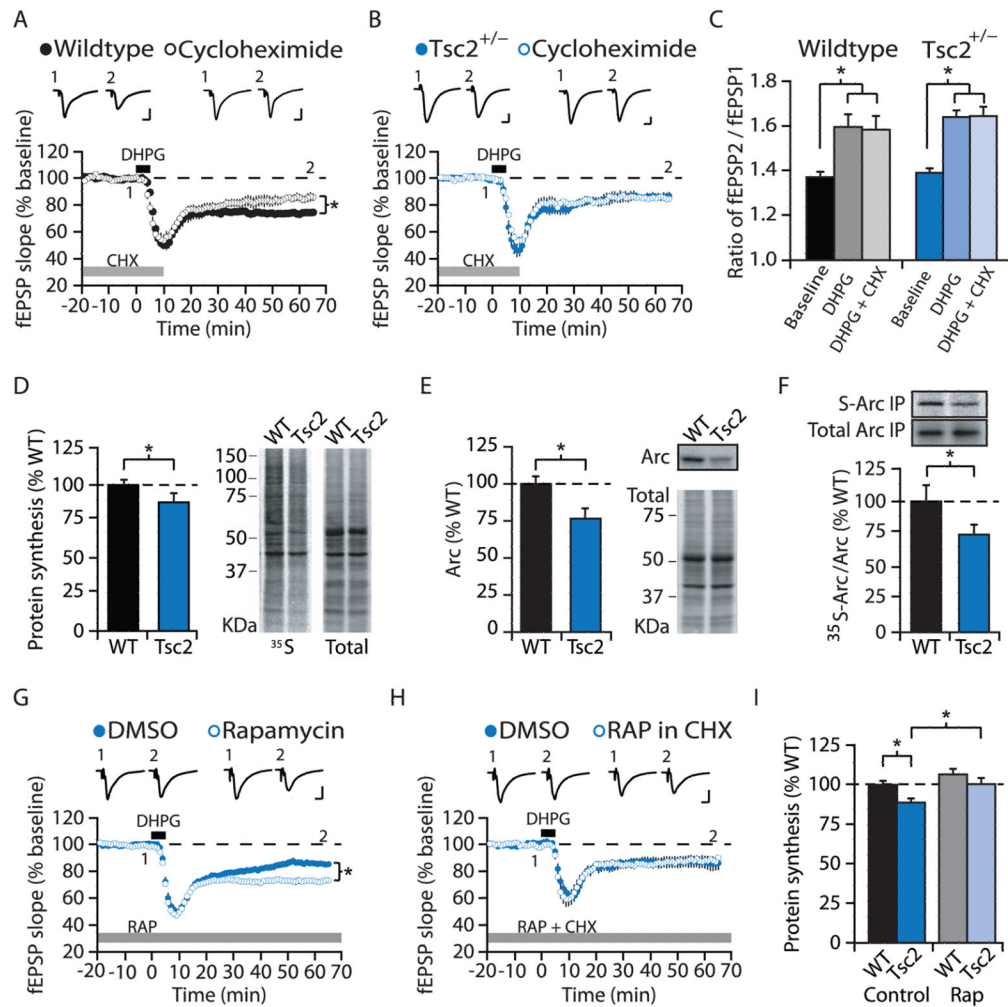


Figure 2. Excessive mTOR activity suppresses the protein-synthesis-dependent component of mGluR-LTD

(A) LTD is significantly attenuated by pretreatment with the protein synthesis inhibitor cycloheximide (CHX, 60 μ M, gray bar) in slices from WT animals (control: $74.3 \pm 1.4\%$, $n = 5$ animals, 10 slices; CHX: $85.2 \pm 2.8\%$, $n = 4$ animals, 7 slices; * $p = 0.014$). (B) CHX treatment has no effect on LTD in slices from *Tsc2*^{+/-} mice (control: $86.3 \pm 3.1\%$, $n = 6$ animals, 12 slices; CHX: $85.3 \pm 3.2\%$, $n = 4$ animals, 7 slices, $p = 0.796$). ANOVA: genotype * $p = 0.041$, treatment $p = 0.089$, genotype \times treatment * $p = 0.045$. (C) Presynaptic LTD is not affected by genotype or CHX (see also Fig. S2). DHPG significantly increased PPF in slices from both WT and *Tsc2*^{+/-} mice (PPF with a 50 ms inter-stimulus interval: WT baseline: 1.37 ± 0.02 , WT DHPG: 1.59 ± 0.06 , $n = 5$ animals, 9 slices, * $p = 0.003$; *Tsc2*^{+/-} baseline: 1.39 ± 0.02 , *Tsc2*^{+/-} DHPG: 1.64 ± 0.03 , $n = 5$ animals, 9 slices, * $p = 0.001$) and this effect was not blocked by CHX (WT DHPG + CHX: 1.58 ± 0.06 , $n = 7$ animals, 11 slices, $p = 0.89$; *Tsc2*^{+/-} DHPG + CHX: 1.64 ± 0.04 , $n = 6$ animals, 7 slices, $p = 0.94$). (D) Metabolic labeling of hippocampal slices reveals a significant reduction of basal protein synthesis in *Tsc2*^{+/-} mice (WT: $100.0 \pm 3.1\%$, *Tsc2*^{+/-}: $88.2 \pm 3.3\%$, $n = 13$ animals; * $p = 0.043$). Differences in protein synthesis are exemplified by representative autoradiograph and total protein stain of the same membrane. (E) Immunoblotting experiments show that Arc expression is significantly reduced in *Tsc2*^{+/-} hippocampal slices (WT: $100.0 \pm 4.7\%$, *Tsc2*^{+/-}: $76.6 \pm 6.4\%$, $n = 12$ animals; * $p = 0.005$). (F) Arc translation

was measured by metabolic labeling of hippocampal slices, followed by immunoprecipitation of Arc. Comparison of the ratios of ^{35}S -incorporated-to-total Arc reveals a significant reduction in Arc translation in the $Tsc2^{+/-}$ hippocampus (WT: $100.0 \pm 11.5\%$, $Tsc2^{+/-}$: $74.7 \pm 6.8\%$, $n = 19$ animals; $*p = 0.049$). **(G)** Pretreatment of slices with the mTORC1 inhibitor rapamycin (RAP, 20 nM, gray bar) significantly enhances DHPG-induced LTD in slices from $Tsc2^{+/-}$ mice (DMSO: $85.7 \pm 2.1\%$, $n = 8$ animals, 17 slices; RAP: $72.9 \pm 1.8\%$, $n = 7$ animals, 18 slices; $*p = 0.002$). **(H)** The rescue by rapamycin of DHPG-induced LTD in $Tsc2^{+/-}$ mice is prevented by the protein synthesis inhibitor cycloheximide (DMSO: $87.1 \pm 4.7\%$, $n = 6$ animals, 10 slices; RAP: $88.1 \pm 2.4\%$, $n = 7$ animals, 9 slices; $p = 0.796$). ANOVA: rapamycin treatment $*p = 0.043$, cycloheximide treatment $*p = 0.004$, rapamycin \times cycloheximide $*p = 0.018$. **(I)** Metabolic labeling experiments show that rapamycin (20 nM) normalizes protein synthesis in the $Tsc2^{+/-}$ hippocampus to WT levels (WT DMSO: $100.0 \pm 2.5\%$, WT RAP: $106.5 \pm 3.6\%$, $Tsc2^{+/-}$ DMSO: $88.8 \pm 2.6\%$, $Tsc2^{+/-}$ RAP: $100.4 \pm 3.9\%$; ANOVA: genotype $*p = 0.008$, treatment $*p = 0.006$, genotype \times treatment $p = 0.430$; t-test: WT vs. $Tsc2^{+/-}$ DMSO $*p = 0.003$; WT vs. $Tsc2^{+/-}$ RAP $p = 0.344$; $Tsc2^{+/-}$ DMSO vs. RAP $*p = 0.037$; $n = 22$ animals). Error bars represent SEM.

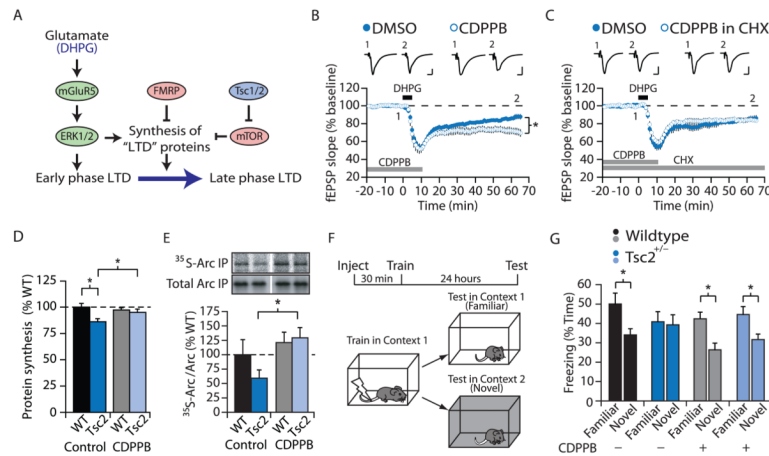


Figure 3. Positive modulation of mGluR5 reverses synaptic and behavioral deficits in *Tsc2*^{+/-} mice

(A) Model to account for effects of *Tsc2*^{+/-} and *Fmr1*^{-/-} mutations on mGluR5- and protein synthesis-dependent LTD. This model predicts that the impairment in *Tsc2*^{+/-} mice can be overcome either by inhibiting mTOR with rapamycin or by augmenting mGluR5 signaling with an mGluR5 PAM. (B) Consistent with the model, pretreatment of slices from *Tsc2*^{+/-} mice with CDPPB (10 μM, gray bar) significantly enhances DHPG-induced LTD (DMSO: 86.4 ± 2.5%, n = 8 animals, 13 slices; CDPPB: 71.7 ± 3.9%, n = 7 animals, 12 slices; *p < 0.001). (C) CDPPB treatment fails to enhance DHPG-induced LTD in *Tsc2*^{+/-} mice when co-applied with the protein synthesis inhibitor cycloheximide (DMSO: 89.0 ± 4.4% n = 8 animals, 10 slices; CDPPB: 83.9 ± 2.1%, n = 7 animals, 9 slices; p = 0.64). ANOVA: CDPPB treatment *p = 0.008, CHX treatment p = 0.087, CDPPB × CHX *p = 0.034. (D) CDPPB (10 μM) restores protein synthesis in the *Tsc2*^{+/-} hippocampus to WT levels (WT DMSO: 100.0 ± 3.2%, WT CDPPB: 97.2 ± 1.9%, *Tsc2*^{+/-} DMSO: 86.1 ± 2.7%, *Tsc2*^{+/-} CDPPB: 94.9 ± 3.0%; ANOVA: genotype *p = 0.006, treatment p = 0.275, genotype × treatment *p = 0.041; t-test: WT vs. *Tsc2*^{+/-} DMSO *p = 0.012; WT vs. *Tsc2*^{+/-} CDPPB p = 0.538; *Tsc2*^{+/-} DMSO vs. CDPPB *p = 0.049; n = 17 animals). (E) CDPPB exposure significantly increases Arc translation in the *Tsc2*^{+/-} hippocampus (WT DMSO 100.0 ± 28.2%, WT CDPPB 121.0 ± 21.2%, *Tsc2*^{+/-} DMSO 59.2 ± 7.0%, *Tsc2*^{+/-} CDPPB 129.4 ± 20.3%; ANOVA genotype p = 0.554, treatment *p = 0.009, genotype × treatment p = 0.114; t-test: *Tsc2*^{+/-} DMSO vs. CDPPB *p = 0.026; n = 6 animals). Error bars represent SEM. (F) Experimental design of context discrimination task. (G) WT mice display intact memory by freezing more in the familiar context than the novel context (Black bars; Familiar: 50 ± 7.7%, n = 12; Novel: 34.1 ± 3.2%, n = 14; *p = 0.003). A single injection of CDPPB (10 mg/kg, i.p.) 30 minutes prior to training has no effect on WT context discrimination (Familiar: 42.3 ± 3.7%, n = 12; Novel: 26.4 ± 3.6%, n = 12; *p = 0.005). Control *Tsc2*^{+/-} mice display an impairment in context discrimination (Blue bars; Familiar: 40.9 ± 5.3%, n = 11; Novel: 39.3 ± 5.2%, n = 14; p = 0.501), but this deficit is corrected by a single injection of CDPPB (Familiar: 44.5 ± 4.3%, n = 11; Novel: 31.6 ± 3%, n = 12; *p = 0.034). Error bars represent SEM.

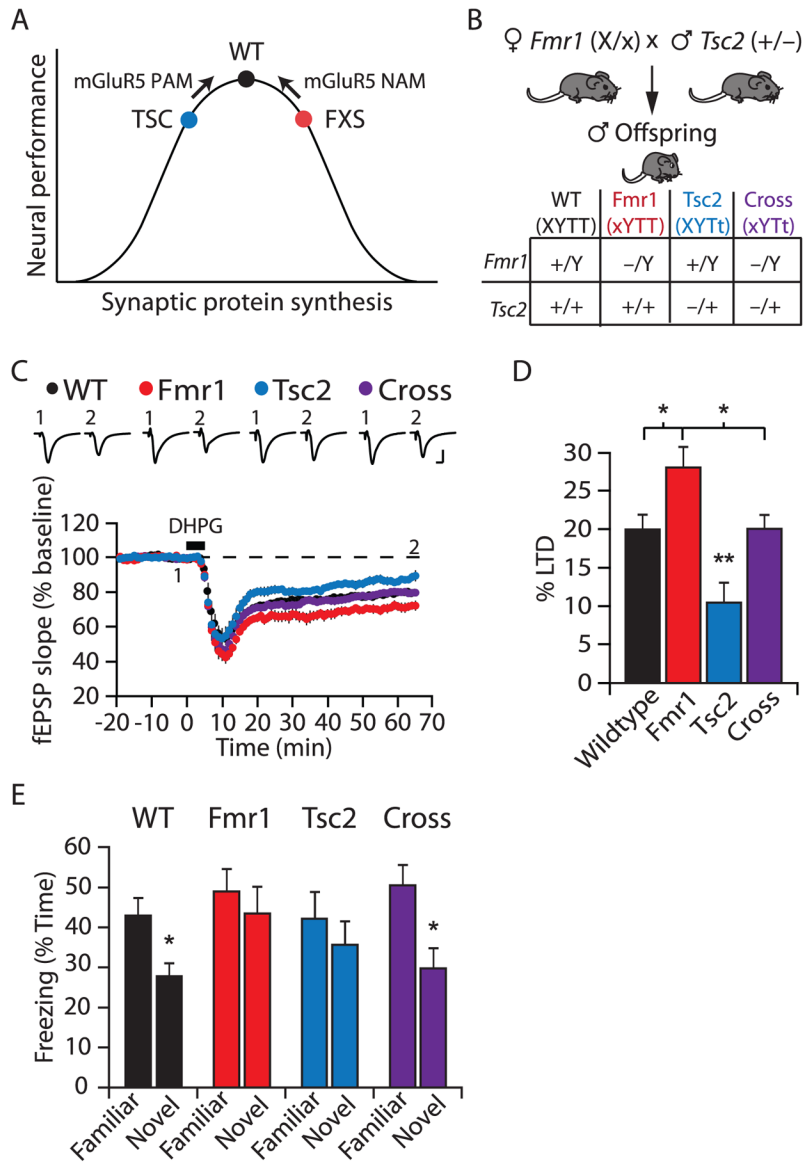


Figure 4. Genetic cross of *Tsc2*^{+/-} and *Fmr1*^{-/-} mice rescues synaptic and behavioral impairments present in both single mutants

(A) The data suggest that optimal synaptic function requires a narrow and tightly regulated level of synaptic protein synthesis and that deviations in either direction can impair function^{3,43}. TSC and FXS fall on different ends of this spectrum and respond to opposite alterations of mGluR5 signaling. These results raise the possibility that introducing both mutations to a mouse may normalize aspects of neural function. (B) Genetic rescue strategy. Heterozygous *Tsc2* male mice (*Tsc2*^{+/-}) were bred with heterozygous *Fmr1* females (*Fmr1* x^{+/x}-) to obtain male offspring of four genotypes: wild type (*Tsc2*^{+/+}, *Fmr1*^{+/y}), *Fmr1* KO (*Tsc2*^{+/+}, *Fmr1*^{-/y}), *Tsc2* Het (*Tsc2*^{+/-}, *Fmr1*^{+/y}), and Cross (*Tsc2*^{+/-}, *Fmr1*^{-/y}). (C) DHPG-induced LTD is significantly decreased in slices from *Tsc2*^{+/-} mice (*p = 0.002) and significantly increased in slices from *Fmr1*^{-/y} mice (*p = 0.017), as compared to WT slices. DHPG-LTD in slices from *Tsc2*^{+/-} × *Fmr1*^{-/y} mice is comparable in magnitude to WT slices (p = 0.558). (WT: 78.9 ± 2.1%, n = 7 animals, 17 slices; *Fmr1*: 71.2 ± 2.7%, n = 7 animals, 21 slices; *Tsc2*: 89.5 ± 2.6%, n = 7 animals, 15 slices; Cross: 77.4 ± 1.8%, n = 9

animals, 19). **(D)** Summary of LTD data. Bar graphs represent percent decrease from baseline in fEPSP (average of last 5 minutes of recording \pm SEM); * $p < 0.05$, ** $p < 0.01$. **(E)** Both mutations cause a deficit in context discrimination that is rescued in the double mutant. WT mice (Familiar: $42.9 \pm 4.6\%$, $n = 11$; Novel: $27.8 \pm 3.4\%$, $n = 12$; * $p = 0.024$), *Fmr1*^{-y} mice (Familiar: $49.0 \pm 5.6\%$, $n = 11$; Novel: $43.5 \pm 6.7\%$, $n = 12$; $p = 0.483$), *Tsc2*^{+/-} (Familiar: $42.1 \pm 6.8\%$, $n = 12$; Novel: $35.6 \pm 6.0\%$, $n = 12$; $p = 0.395$) and *Tsc2*^{+/-} x *Fmr1*^{-y} mice (Familiar: $50.5 \pm 5.2\%$, $n = 11$; Novel: $29.8 \pm 5.2\%$, $n = 11$; * $p = 0.011$). Error bars represent SEM.